Four-wave polarization interaction in photorefractive crystals

S. G. Odulov and B. I. Sturman

Institute of Automation and Electrometry, Siberian Branch of the Academy of Sciences of the USSR, Novosibirsk

(Submitted 11 November 1986)
Zh. Eksp. Teor. Fiz. **92**, 2016–2033 (June 1987)

A frequency-degenerate four-wave polarization interaction in photorefractive crystals is investigated. This interaction is due to linear and circular photogalvanic currents and couples light beams with orthogonal polarizations. The properties of this interaction differ from that associated with the drift and diffusion of photoelectrons. The nonlinear equations are solved exactly for various experimental configurations. A study is made of the characteristics of phase conjugation. It is shown that the solutions are bistable when the nonlinearity is sufficiently strong and the distinguishing characteristics of the nonlinearity are determined. Studies are made of lasing due to the polarization interaction in the presence and absence of mirrors. Experiments on $LiNbO_3$:Fe crystals are reported; they provide qualitative confirmation of the main theoretical ideas. The new effects are comparable in magnitude with those known previously.

INTRODUCTION

A giant optical nonlinearity, which can give rise to values of the gain in the range $1–10^2$ cm^{-1} in interactions of light beams of intensities down to 10^{-6} W/cm^2, exhibited by photorefractive crystals ($LiNbO_3$, $BaTiO_3$, etc.) with a quadratic nonlinearity of the refractive index has made these crystals the object of intensive investigations.[1–4] Experimental and theoretical studies have been made of the nonlinearity and of its various manifestations, particularly in phase conjugation.[5]

It has been found that spatial modulation of the optical-frequency permittivity $\Delta\varepsilon(r)$, responsible for the interaction, is associated with charge separation because of the drift of inhomogeneously excited carriers in an external field,[6] their diffusion,[7] and photogalvanic effect.[8–10] From the phenomenological point of view the optical phenomena observed in photorefractive crystals can be regarded as a manifestation of a frequency–degenerate four-wave interaction.

It has been found that a very effective approach in theoretical and experimental studies is provided by considering elementary nonlinear optical processes representing the interaction of two plane waves and the diffraction of light by a grating $\Delta\varepsilon(\mathbf{r})$ formed by these waves. An analysis of the dependences of the gain and of the diffraction efficiency on time, angle of convergence of light beams, their orientations, and the ratios of the intensities has made it possible to obtain detailed information on the mechanisms responsible for charge transport and on the fundamental parameters of crystals.[2] The feasibility of numerous applications has been demonstrated.[4] An important feature of these investigations has also been the interaction of four waves in phase conjugation systems.[3,5] Photorefractive crystals are among the most convenient and promising materials for this application.

A great majority of the studies carried out so far have been confined to waves of one type: ordinary (o) or extraordinary (e). In this situation the effect of each of the three nonlinearity mechanisms—drift, diffusion, and photogalvanism—is related directly to spatial modulation of the intensity of light.

Photorefractive crystals provide a unique opportunity for investigating a giant nonlinear interaction of waves with orthogonal polarizations, o and e waves. In this case the intensity of light is not modulated and the charge separation by drift and diffusion is impossible. The modulation of $\Delta\varepsilon(\mathbf{r})$ is due to specific photocurrents which oscillate in space and travel along directions that depend on the state of polarization of light and not on its intensity.[9,11] Such currents always accompany the photogalvanic effect. The polarization interaction of o and e waves and the writing of holographic gratings of $\Delta\varepsilon(\mathbf{r})$ by these waves were predicted in Ref. 12 and the experimental confirmation of these effects was first given in Ref. 13.

The present paper describes an investigation of the four-wave polarization interaction in photorefractive crystals. The nonlinear equations describing the spatial behavior of the wave amplitudes are structurally different from those considered earlier,[3] which is a manifestation of the gyrotropy of a crystal affecting optical properties. In spite of the non-Hamiltonian nature of the interaction of the waves, these equations include a number of quantities which are conserved. They can be used to find the general solution of the nonlinear system of equations and to analyze in detail this solution in the case of specific experimental configurations. It is found that manifestations of the polarization interaction in two-beam interaction configurations, in phase conjugation, and in optical lasing are qualitatively different from those considered earlier. Experiments on $LiNbO_3$ crystals are reported: they confirm qualitatively the main theoretical propositions and show that the magnitudes of the new effects are comparable with the already known effects associated with the diffusion-drift nonlinearity.

§1. PHOTOGALVANIC NONLINEARITY MECHANISM

Let us assume that o and e waves of the same frequency propagate in the plane of a crystal perpendicular to the polar **c** axis (Fig. 1a). The complex amplitude of the field is given by

$$\mathbf{E}=\exp(-i\omega t)[\mathbf{e}_o a_o \exp(i\mathbf{k}_o\mathbf{r})+\mathbf{e}_e a_e \exp(i\mathbf{k}_e\mathbf{r})], \quad (1.1)$$

where $\mathbf{e}_{o,e}=\mathbf{e}^*_{o,e}$ are unit vectors of the polarization. The

 0038-5646/87/061134-11$04.00 © 1987 American Institute of Physics

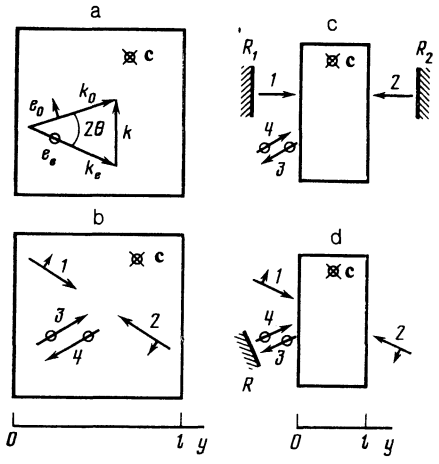

FIG. 1. Experimental configurations used in the study of the polarization interaction of o and e waves: a) two-beam interaction; b) opposed four-wave interaction (reversing mirror); c) lasing in a linear resonator with one pump wave (self-pumped reversing mirror); d) lasing in a semilinear resonator with two pump beams.

change in the permittivity tensor responsible for the interaction is

$$\Delta\varepsilon_{z\mu}(\mathbf{r})=\Delta\varepsilon_{z\mu}\exp\left[i(\mathbf{k}_o-\mathbf{k}_e)\mathbf{r}\right]+\text{c.c.},\quad \mu=x,\ y. \tag{1.2}$$

In view of the orthogonality of $\mathbf{e}_o$ and $\mathbf{e}_e$, the total light intensity does not exhibit spatial oscillations with $\mathbf{k}=\mathbf{k}_o-\mathbf{k}_e$. Therefore, neither the diffusion of photocarriers nor their drift in an external field contributes to the formation of a grating of $\Delta\varepsilon(\mathbf{r})$. However, the photocurrent associated with the photogalvanic effect has a spatially oscillating component, which is responsible for the interaction. The general phenomenological expression for the current is[9]

$$j_\alpha=\beta_{\alpha\beta\gamma}E_\beta E_\gamma^*, \tag{1.3}$$

where $\beta_{\alpha\beta\gamma}=\beta^*_{\alpha\gamma\beta}$ is the photogalvanic tensor. Not all the components of $\hat{\beta}$ give rise to spatial oscillations of the current in our geometry. In crystals of C_{3v}, C_{4v}, C_{6v} classes (and practically all the photorefractive ferroelectrics belong to these classes) the interaction is due to the following component of the current:

$$\mathbf{j}=\beta_s\{(\mathbf{cE})\mathbf{E}^*+(\mathbf{cE})^*\mathbf{E}\}+i\beta_a[\mathbf{c}[\mathbf{EE}^*]]. \tag{1.4}$$

Here, $\beta_{s,a}$ are independent components of the photogalvanic tensor described by $\beta_s=(\beta_{131}+\beta_{113})/2$, and $\beta_a=-i(\beta_{113}-\beta_{131})/2$. The constant β_a of a photorefractive material is associated with the gyrotropic properties of the medium; the corresponding contribution to $\mathbf{j}$ we call circular.[9] Using Eq. (1.1), we find from Eq. (1.4) that

$$\mathbf{j}=2\mathbf{e}_o|a_oa_e|\left[\beta_s\cos(\mathbf{kr}+\varphi)-\beta_a\sin(\mathbf{kr}+\varphi)\right],\qquad \varphi=\varphi_o-\varphi_e, \tag{1.5}$$

where $\varphi_{o,e}$ are the phases of the o and e waves. It follows from Eq. (1.5) that oscillations of the current (and of $\Delta\varepsilon$) governed by β_s and β_a are phase-shifted relative to one another by $\pi/2$. The s and a spatial gratings can be regarded as unshifted and shifted, respectively. These gratings correspond respectively to the local and nonlocal nonlinear response of the medium.[2]

We shall now calculate the change in the permittivity $\Delta\varepsilon_{z\mu}$, induced by the current of Eq. (1.5). It can be expressed in terms of the electrostatic field $\mathscr{E}(r)=\mathscr{E}\exp(i\mathbf{kr})+\text{c.c.}$ and in terms of the constant r_{51} of the linear electrooptic effect[2,12]:

$$\Delta\varepsilon_{z\mu}=-n^4r_{51}\mathscr{E}_\mu, \tag{1.6}$$

where n is the refractive index. We shall ignore the small corrections associated with birefringence. In the determination of $\vec{\mathscr{E}}$ we must bear in mind that only the component of $\mathbf{j}$ parallel to the lattice vector $\mathbf{k}$ is responsible for the charge separation process. Therefore, we have $\vec{\mathscr{E}}=\mathbf{s}\mathscr{E}$, $\mathbf{s}=\mathbf{k}/k$, and

$$\frac{\partial\mathscr{E}}{\partial t}+\frac{\mathscr{E}}{t_d}=-\frac{4\pi}{\varepsilon_\perp}(\beta_s+i\beta_a)(\mathbf{se}_o)a_oa_e^*, \tag{1.7}$$

where $t_d=\varepsilon_\perp/4\pi\sigma$ is the dielectric relaxation time. In the milliwatt range of optical powers typical values of t_d lie within the range $10^{-1}-10^2$ sec; σ is the electrical conductivity (including the photoconductivity); $\varepsilon_\perp$ is the transverse static permittivity. Under steady-state conditions, we have

$$\mathscr{E}=-\sigma^{-1}(\beta_s+i\beta_a)(\mathbf{se}_o)a_oa_e^*. \tag{1.8}$$

We must mention two factors which distinguish the optical system shown in Fig. 1a from conventional ones[2,3]: 1) the conductivity σ does not experience spatial oscillations; 2) there is no spatially uniform component of $\mathscr{E}_\mu$. This enables us to obtain the above simple relationships (1.7) and (1.8) without additional assumptions about the low intensity of one of the light beams and about the nature of the boundary conditions (insulated or short-circuited crystal).

The material equations (1.6)–(1.8) describe the nonlinear response of a photorefractive medium. Equations for the amplitudes of light waves are obtained from the Maxwell equations by going over to envelopes in the usual manner. The time derivatives of $a_{o,e}$ can then be ignored for all practical cases. This means that the light "follows" the adiabatically slow changes of $\Delta\hat{\varepsilon}(t)$. Calculations then give[12]

$$\begin{aligned}(\mathbf{k}_o\nabla)a_o&=-(i\omega^2/2c^2)n^4r_{51}(\mathbf{e}_o\mathbf{s})\mathscr{E}a_e,\\ (\mathbf{k}_e\nabla)a_e&=-(i\omega^2/2c^2)n^4r_{51}(\mathbf{e}_o\mathbf{s})\mathscr{E}^*a_o.\end{aligned} \tag{1.9}$$

Equations (1.7) and (1.9) form a closed system. It follows directly from Eq. (1.9) that $\operatorname{div}(\mathbf{k}_o|a_o|^2+\mathbf{k}_e|a_e|^2)=0$, which is the law of conservation of energy.

Under steady-state conditions we find from Eqs. (1.8) and (1.9) that

$$(\mathbf{k}_o\nabla)a_o=iF|a_e|^2a_o/2,\qquad (\mathbf{k}_e\nabla)a_e=iF^*|a_o|^2a_e/2, \tag{1.10}$$

where

$$F=F'+iF''=\frac{\omega^2}{c^2}\frac{n^4r_{51}}{\sigma}(\beta_s+i\beta_a)(\mathbf{e}_o\mathbf{s})^2 \tag{1.11}$$

represents a coupling constant.

The general nature of the system (1.10) is naturally the same as in the case of the two-wave interaction due to drift and diffusion.[2] Energy transfer results from the photogalvanic constant β_a describing the circular photogalvanic effect. Under steady-state conditions the constant β_s is solely responsible for the "phase pumping." The solution of the system (1.10) obtained for the geometry in Fig. 1a gives the standard expressions[2] for the wave intensities:

$$|a_{o,e}|^2=\frac{|a_o(0)|^2+|a_e(0)|^2}{1+m^{\pm 1}\exp(\pm\Gamma y)},\qquad m=\left|\frac{a_e(0)}{a_o(0)}\right|^2. \tag{1.12}$$

The quantity Γ represents the gain:

$$\Gamma=\frac{F''(|a_o(0)|^2+|a_e(0)|^2)}{k\cos\theta}=\frac{\omega}{c}\frac{n^3r_{51}\beta_a(\mathbf{e}_0\mathbf{s})^2(|a_o(0)|^2+|a_e(0)|^2)}{\sigma\cos\theta}. \tag{1.13}$$

We can see from Eq. (1.12) that the direction of energy exchange is independent of the ratio of the beam intensities (unidirectional energy exchange). If a weak beam is amplified, its growth is exponential.

The differences between the photogalvanic mechanism and the diffusion and drift mechanisms are associated with the dependences of F and Γ on the orientation of the $\mathbf{c}$ polar axis, and on the polarization and angle of convergence of the beams. It follows from Eqs. (1.11) and (1.12) that the reversal of the polar axis $\mathbf{c}\to-\mathbf{c}$ does not alter the direction of energy exchange, because $\beta_{s,a}\to-\beta_{s,a}$ and $r_{51}\to-r_{51}$. The direction of steady-state energy exchange is governed by the sign of the product $r_{51}\beta_a$. If $r_{51}\beta_s>0$, energy is transferred from an ordinary to an extraordinary wave, whereas for $r_{51}\beta_a<0$ the transfer is from an extraordinary to an ordinary wave. In the diffusion mechanism the reversal of the direction of the polar axis $\mathbf{c}\to-\mathbf{c}$ alters the direction of energy exchange.[2] When the polarizations are reversed in accordance with $o\rightleftarrows e$, we find that $F\to F^*$.

The dependence of the coupling constant F and of the gain Γ on the angle 2θ between $\mathbf{k}_o$ and $\mathbf{k}_e$ is given by the expression

$$(\mathbf{se}_o)^2=\sin^2(2\theta)[(\Delta n/n)^2+4\sin^2\theta]^{-1}, \tag{1.14}$$

where $\Delta n/n\ll 1$ is the birefringence of the investigated crystal. Allowance for the birefringence is essential only in the range of small angles $2\theta\lesssim|\Delta n/n|$, where $(\mathbf{se}_o)^2\approx(2n\theta/\Delta n)^2$; outside this range we have $(\mathbf{se}_o)^2\approx\cos^2\theta$. Therefore, the opposed or antiparallel interaction $[(\pi/2)-\theta\ll 1]$ is weak compared with that in the parallel or concurrent direction ($\theta\ll 1$). This is also an important distinguishing feature of the photogalvanic nonlinearity mechanism.

In addition to the steady-state regime, there is a considerable interest in the initial stage of kinetics, when $t\ll t_d$, during which the field rises linearly with time:

$$\mathscr{E}\approx-\frac{4\pi}{\varepsilon_\perp}(\beta_s+i\beta_a)(\mathbf{se}_o)a_oa_e^*t. \tag{1.15}$$

The results of optical measurements carried out during this stage can yield directly the photogalvanic constants β_s and β_a. Assuming that the nonlinear phase shifts in the length of a crystal l are small, we find from Eqs. (1.9) and (1.15) the change in the intensities

$$\delta|a_e|^2=-\delta|a_o|^2=\frac{8\pi^2n^3r_{51}\beta_a(\mathbf{se}_o)^2}{\varepsilon_\perp\lambda_0\cos\theta}|a_oa_e|^2lt, \tag{1.16}$$

where λ_0 is the wavelength of light in vacuum. Therefore, measurements of $\delta|a_{o,e}|^2$ can yield directly the constant β_a.

If at time t one of the beams is interrupted, the second beam is diffracted by a grating of $\Delta\varepsilon(t)$ and this is accompanied by rotation of the plane of polarization. The diffraction efficiency $\eta(t)\equiv|\delta a/a|^2$ deduced from Eqs. (1.9) and (1.15) is

$$\eta=\frac{(2\pi)^4(\mathbf{e}_o\mathbf{s})^4n^6r_{51}^2}{\varepsilon_\perp^2\lambda_0^2\cos^2\theta}|a_oa_e|^2l^2t^2(\beta_s^2+\beta_a^2). \tag{1.17}$$

Determination of η yields $\beta_s^2+\beta_a^2$. It should be pointed out that Eqs. (1.16) and (1.17) do not contain the conductivity σ of the medium.

On the whole, Eqs. (1.7) and (1.9) describing the kinetics of the two-beam energy exchange are simpler than in the case of the drift and diffusion mechanisms.[14,15] This is due to the absence of a constant (in $\mathbf{r}$) component of the field and of an oscillatory photoconductivity. However, the qualitative behavior of $|a_{o,e}(t)|^2$ remains the same as in the drift and diffusion mechanisms. If $\beta_a\gg\beta_s$, then the steady state described by Eq. (1.12) is attained in a monotonic manner. If $\beta_s\gg\beta_a$, the unidirectional nature of energy exchange is manifested only after a long time $t\gg t_d$. Before this happens the intensities $|a_{o,e}(l)|^2$ exhibit oscillations in time associated with β_s and representing energy transfer from a strong to a weak beam; during the initial stage, $t<t_d$, the weak beam grows quadratically with time. An analytic investigation can be carried out only in certain special cases (see Ref. 15).

§2. OPPOSED FOUR-WAVE INTERACTION

We shall now derive a system of equations describing the interaction of four waves representing two pairs of oppositely directed o and e waves (Fig. 1b). This system is obtained by generalization of the equations for two waves. Pairs of waves 1, 4 and 2, 3 are formed by gratings of $\Delta\hat{\varepsilon}(\mathbf{r})$ with identical vectors $\mathbf{k}=\mathbf{k}_1-\mathbf{k}_4=\mathbf{k}_3-\mathbf{k}_2$ (transmission gratings). These gratings determine the interaction. Reflection gratings with the vectors $\mathbf{k}_1-\mathbf{k}_3=\mathbf{k}_2-\mathbf{k}_4$, responsible for the opposed interaction, will be ignored on the assumption that $\theta^2\ll 1$ (this condition is well satisfied in experiments). Using Eqs. (1.6) and (1.7), we can write down the equation which describes the grating amplitude $\mathscr{E}$. It will be convenient to use the following quantity, which is in one-to-one correspondence with this amplitude:

$$G=-i\omega^2n^4r_{51}(\mathbf{e}_o\mathbf{s})\mathscr{E}/2kc^2\cos\theta. \tag{2.1}$$

We can easily see that

$$(\partial/\partial\tau+1)G=i(Fa_1a_4^*+F^*a_2^*a_3)/2k\cos\theta, \tag{2.2}$$

where F is still given by Eq. (1.11) and the dimensionless time is $\tau=t/t_d$. Note that the contribution of the pair of waves 2, 3 is characterized by the complex-conjugate coupling constant $F^*\propto\beta_s-i\beta_a$. This is related directly to the presence of the circular component of the current described by Eq. (1.4), i.e., to the gyrotropic properties of the medium. It can be explained as follows: the grating vector $\mathbf{k}=\mathbf{k}_3-\mathbf{k}_2$ corresponds to the combination $a_3a_2^*$, in which (compared with $a_1a_4^*$) the o and e waves are transposed. However, it follows from Eq. (1.4) that transposition of two orthogonal polarization vectors in a vector product reverses the sign of the circular current. In other words, we can say that the contributions made to the circular current by $a_1a_4^*\exp(i\mathbf{kr})$ and $a_3a_2^*\exp(i\mathbf{kr})$ have to be subtracted.

The equations for the amplitudes of the waves follow in

an elementary manner from Eq. (1.9). In the geometry of Fig. 1b they are written in the form

$$\partial a_1/\partial y=Ga_4, \quad \partial a_2^*/\partial y=Ga_3^*,$$
$$\partial a_3/\partial y=-Ga_2, \quad \partial a_4^*/\partial y=-Ga_1^*. \tag{2.3}$$

Equations (2.2) and (2.3) form a closed system. Under steady-state conditions we can describe G explicitly in terms of the wave amplitudes:

$$G=i[Fa_1a_4^*+F^*a_2^*a_3]/2k\cos\theta. \tag{2.4}$$

It should be stressed that Eqs. (2.2)–(2.4) do not reduce to the equations describing the four-wave interaction due to drift and diffusion.[3] The difference is associated with the imaginary part of the coupling constant F, i.e., it is due to the circular photogalvanic effect. We shall show later that this difference gives rise to several new physical effects.

We can easily show that the system (2.3) contains quantities Σ, $d_{1,2}$, c, c_2 which are conserved:

$$\begin{aligned} &|a_1|^2+|a_2|^2+|a_3|^2+|a_4|^2=\Sigma,\\ &|a_1|^2+|a_4|^2=d_1\Sigma, \quad |a_2|^2+|a_3|^2=d_2\Sigma,\\ &a_1a_2+a_3a_4=c\Sigma, \quad a_1a_3^*-a_2^*a_4=c_2\Sigma. \end{aligned} \tag{2.5}$$

Apart from normalization, these quantities are identical with the integrals of motion of Ref. 3. The quantities Σ, $d_{1,2}$, c, c_2 can generally be functions of time. They are not completely independent because $d_1+d_2=1$ and $|c|^2+|c_2|^2=d_1d_2$. The quantity Σ can be regarded as the total intensity of light in a crystal, whereas $d_{1,2}$ are the total intensities of the beams traveling to the right and left, normalized to Σ.

Under steady-state conditions we can use Eq. (2.5) to reduce the order of the system (2.3) and to obtain its exact solution. Following Ref. 3, we shall replace $a_{1,2,3,4}$ with two complex quantities:

$$A_{12}=a_1/a_2^*, \quad A_{34}=a_3/a_4^*. \tag{2.6}$$

The knowledge of A_{12} and A_{34} allows us to reconstruct the intensities of all the beams.[3] Using Eqs. (2.3)–(2.6), we obtain two independent equations:

$$\begin{aligned} dA_{12}/dy&=i[F^*c+(Fd_1-F^*d_2)A_{12}-Fc^*A_{12}^2]/2k\cos\theta,\\ dA_{34}/dy&=-i[Fc+(F^*d_2-Fd_1)A_{34}-F^*c^*A_{34}^2]/2k\cos\theta. \end{aligned} \tag{2.7}$$

The general solution of Eq. (2.7) is

$$\begin{aligned} A_{12}&=\frac{S_+-S_-D_{12}\exp(2\mu y)}{2Fc^*[1-D_{12}\exp(2\mu y)]},\\ A_{34}&=-\frac{S_+-S_-D_{34}\exp(2\mu y)}{2F^*c^*[1-D_{34}\exp(2\mu y)]}, \end{aligned} \tag{2.8}$$

where

$$\begin{aligned} &S_\pm=P\pm(P^2+4|Fc|^2)^{1/2}, \quad P=Fd_1-F^*d_2,\\ &\mu=-i(P^2+4|Fc|^2)^{1/2}/4k\cos\theta, \end{aligned} \tag{2.9}$$

and D_{12} and D_{34} are the constants of integration. Together with the constants c and $d_{1,2}$, they should be determined using specific boundary conditions. The problem is thus reduced to a system of algebraic equations.

We shall later find it convenient to use the following notation:

$$\Omega=F''\Sigma/k\cos\theta, \quad \Gamma=F''\Sigma/k\cos\theta, \quad I_j=|a_j|^2/\Sigma, \quad \Delta=d_2-d_1, \tag{2.10}$$

where Γ and Ω are, respectively, the gain and the nonlinear frequency shift; $I_{1,2,3,4}$ are the normalized dimensionless beam intensities; Δ can be regarded as the relative difference between the energy fluxes. The expression (2.10) for Γ reduces to Eq. (1.13) in the two-wave interaction case.

§3. REVERSING MIRROR

Let us assume that three waves, 1, 2, and 4, are incident on a crystal (Fig. 1b). The boundary conditions corresponding to this case are

$$I_{1,4}(0)=I_{1,4}, \quad I_2(l)=I_2^l, \quad I_3(0)=0. \tag{3.1}$$

Clearly,

$$I_1^0+I_2^l+I_4^0=1, \quad d_1=I_1^0+I_4^0, \quad d_2=I_2^l, \quad \Delta=2I_2^l-1.$$

If we use Eqs. (2.8) and (3.1) to find the integration constant D_{34}, we obtain the following relationship for the ratio of the amplitudes of the reversed (3) and signal (4) waves:

$$A_{34}(0)=2Fc[P-(P^2+4|Fc|^2)^{1/2}\operatorname{cth}(\mu l)]^{-1}. \tag{3.2}$$

Next, we can find D_{12} making use of the relation $A_{12}(l)=c/I_2^l$. Finally, the identity $A_{12}(0)=I_1^0[c^*-A_{34}^*(0)I_4^0]^{-1}$ and some transformations yield the following real algebraic equation:

$$\begin{aligned} &4I_1^0I_4^0|F|^2|\Phi|^2+|(P-2FI_4^0)\Phi-1|^2=\frac{I_1^0I_2^l}{|c|^2}|P\Phi-1|^2;\\ &\Phi\equiv\frac{\operatorname{th}(\mu l)}{(P^2+4|Fc|^2)^{1/2}}. \end{aligned} \tag{3.3}$$

It describes an auxiliary quantity $|c|^2$, important in subsequent analysis, as a function of I_1^0, I_2^l, I_4^0 Γl, Ωl. If the interaction constant is real ($\Gamma=0$), the system (3.3) is identical with the corresponding equation in Ref. 3. When we know $|c|^2$, we can calculate the intensities of all the waves. The system (3.3) taken as a whole is very complicated, so that we shall consider only the most important limiting cases.

Approximation of a constant field of pump waves

If $I_4^0=0$, there is obviously a solution corresponding to two noninteracting pump waves:

$$I_{3,4}=0, \quad I_1(y)=I_1^0, \quad I_2(y)=I_2^l, \quad |c|^2=I_1^0I_2^l.$$

Therefore, if the intensity of the signal wave obeys $I_4^0\ll I_1^0$, I_2^l and the medium l is sufficiently thin (the criterion for thinness will be given later), we can use the constant-pump-wave approximation and assume that

$$P=(-\Omega\Delta+i\Gamma)/2, \quad \mu=-(\Gamma\Delta+i\Omega)/4.$$

Equation (3.2) yields the explicit expression for the experimentally observed quantity, which is the reflection coefficient of a reversed wave $M_{34}=|a_3(0)/a_4(0)|^2$:

$$M_{34}=\frac{(\Gamma^2+\Omega^2)(1-\Delta^2)}{|(\Gamma+i\Omega\Delta)-(\Gamma\Delta+i\Omega)\operatorname{cth}[(\Gamma\Delta+i\Omega)l/4]|^2}. \tag{3.4}$$

If $\Gamma\Delta l\ll 1$ and $\Omega l\ll 1$, this coefficient is given by

$$M_{34}=(\Gamma^2+\Omega^2)(1-\Delta^2)l^2[(\Gamma l-4)^2+\Omega^2\Delta^2 l^2]^{-1}. \quad (3.5)$$

For brevity, we shall call M_{34} the reversal coefficient. It is worth noting the divergence of M_{34} for $\Omega\Delta\to 0$ and $\Gamma l\to 4$. There is no such divergence in the diffusion mechanism of the nonlinearity.[3] In the case of a purely nonlocal response ($\Omega=0$) the divergence occurs even for finite values of Δ:

$$M_{34}=(1-\Delta^2)[1-\Delta\,\mathrm{cth}\,(\Gamma\Delta l/4)]^{-2}. \quad (3.6)$$

It should be noted that Eqs. (3.5) and (3.6) represent even functions of Δ. Variation of $|\Delta|$ from zero to unity increases the critical value $\Gamma l/4$ from unity to infinity. The singularity (divergence) of M_{34} is retained also for $\Omega\neq 0$ if $\Delta=0$; it corresponds to $\Gamma=\Omega\cot(\Omega l/4)$. The rise of $|\Omega|$ reduces $(\Gamma l)_{cr}$.

Naturally, near such a singularity the constant pumping approximation is invalid. However, the very existence of $(\Gamma l)_{cr}$ is an indication of bifurcation of the solution. This bifurcation is due to the possibility of lasing. In this case the noninteracting *o* waves 1 and 2 serve as the pump waves, and the *e* waves 3 and 4 appear spontaneously inside a crystal only if $\Gamma l>(\Gamma l)_{cr}$; the intensities of the incident waves are $I_3^l=I_4^0=0$. The equation

$$\mathrm{th}\,(\Gamma l\Delta/4)_{cr}=\Delta, \quad (3.7)$$

corresponding to a singularity of M_{34} at $\Omega=0$ should be regarded as the lasing threshold. Lasing is also possible if $\Omega\neq 0$ and $\Delta=0$. When pumping is provided by the beams 2 and 4, there is no singularity of $M_{34}=I_3(0)/I_4^0$ and lasing is impossible.

Note that in the diffusive nonlinear response a divergence of M_{34} does not appear and lasing is impossible. The principal difference between the photogalvanic nonlinearity mechanism and the diffusive mechanism is due to the feature mentioned above, which is the phase-synchronizing nature of the gratings of $\Delta\hat{\varepsilon}(\mathbf{r})$ created by the pairs of waves 1, 4 and 2, 3 (see also Ref. 16).

An investigation of the state above the lasing threshold and of the reversal coefficient M_{34} will be made below on the basis of the exact equation (3.3) without recourse to the constant-pumping approximation.

Stationary states in the case of a nonlocal response

If $\Omega=0$, Eq. (3.3) can be written in the form

$$\frac{(\Phi-1)^2}{\Phi(I_2^l\Phi-1)}=\frac{4|c|^2I_4^0}{|c|^2-I_1^0I_2^l}, \qquad \Phi=\frac{\mathrm{th}\,(f\Gamma l/4)}{f},$$
$$f=(1-4|c|^2)^{1/2}. \quad (3.8)$$

We shall investigate the behavior of $|c|^2$ as a function of the nonlinear parameter $x=\Gamma l/4$. Graphical analysis of Eq. (3.8) establishes that there always is a main branch $|c(x)|^2$, which decreases monotonically from the finitie value to zero as x increases from $-\infty$ to ∞. We can also show that if $|x|$ is sufficiently large, there may be an additional double-valued branch which does not intersect the main branch. Therefore, there can be three solutions for the same boundary conditions (3.1).

The asymptotic behavior of $|c|^2$ in the limit $|x|\to\infty$ and the conditions for the appearance of an additional branch can be determined analytically. Let us assume that $\Gamma l=\infty$ and $4|c|^2\neq 1$ ($f\neq 0$). Then, if $\tanh(fx)=1$, Eq. (3.8) yields the following fourth-degree equation for f:

$$(f-1)(f-\Delta)[(f-1)(f+\Delta)+4I_4^0 f]=0. \quad (3.9)$$

The solution of Eq. (3.9) given by $f^{(0)}=1$ ($|c|^2=0$) corresponds to the main branch. The nature of the approach of $|c^2|$ to zero in the limit $\Gamma l\to\infty$ can be found more accurately using Eq. (3.8):

$$|c|^2\simeq I_1^0I_2^l[I_4^0(1-I_2^l)]^{-1}\exp(-4x). \quad (3.10)$$

In the case of the additional solutions of Eq. (3.9) we can easily see that either two or none are real and positive. If $\Delta>0$, there is always a pair of positive roots $f^{(1)}=I_1^0-I_4^0+[(I_1^0-I_4^0)^2+\Delta]^{1/2}$, and $f^{(2)}=\Delta$. If the signal wave 4 is weak, $I_4^0\ll I_1^0$, I_2^l, then $f^{(1)}\simeq 1-2I_4^0/I_2^l$. If $\Delta<0$, then the positive roots $f^{(1,2)}=I_1^0-I_4^0\pm[(I_1^0-I_4^0)^2+\Delta]^{1/2}$ exist only in the range defined by the inequality $2(I_4^0)^{1/2}\leqslant 1-|\Delta|^{1/2}$. In the limit $\Delta\to -1$ this range contracts to a point: $I_4^0\to 0$, and $I_1^0\to 0$. If the wave 4 is weak, then $f^{(1)}$ is still given by $1-2I_4^0/I_2^l$, and we also have $f^{(2)}=-\Delta$.

We shall now consider the behavior of $|c|^2$ in the limit $x\to-\infty$. The equation for f is obtained from Eq. (3.9) by the substitution $f\to -f$. It then follows that if $\Delta>0$, there is one positive root $f^{(0)}=I_4^0-I_1^0+[(I_1^0-I_4^{02}+\Delta]^{1/2}$ corresponding to the main branch. If $\Delta<0$, we know there is a solution $f=|\Delta|$. If the additional condition $2(I_1^0)^{1/2}<1-|\Delta|^{1/2}$ is satisfied, there are further positive roots $f=I_4^0-I_1^0\pm[(I_1^0-I_4^0)^2+\Delta]^{1/2}$. If the wave 1 being amplified is weak, we find that in the case of the main branch we have $f^{(0)}=1-2I_1^0/I_2^l$, whereas for the additional branches we have $f^{(1)}=|\Delta|$ and $f^{(2)}\simeq|\Delta|(1-2I_1^0/I_2^l)$,

The domains in which the various regimes exist are plotted in Fig. 2. The condition for the appearance of multivalued solutions implies qualitatively that the signal wave should be the one which is amplified and it should be fairly weak.

We now consider the behavior of the solutions of Eq. (3.8) in the case of intermediate values of the nonlinear parameter $x=\Gamma l/4$. Figure 3 shows typical results of numerical calculations demonstrating the behavior of the branches of $|c(x)|^2$.

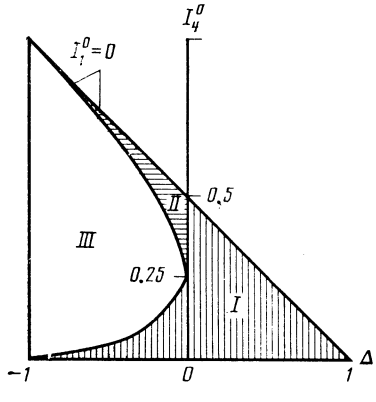

FIG. 2. Ranges of the input parameters corresponding to single-valued and multivalued stationary states: I) $\Gamma>0$, triple-valued solution; II) $\Gamma<0$, triple-valued solution; III) single-valued solution.

If $\Gamma > 0$, then for a fixed value of Δ we find that $x_{cr} = (\Gamma l)_{cr}/4$ corresponding to the appearance of an additional branch decreases on reduction in I_4^0. In the limit $I_4^0 \to 0$, corresponding to lasing x_{cr} is given by Eq. (3.7). If $I_4^0 = 0$ and $\Delta = 0$, then $x_{cr} = 1$. This is the minimum threshold (corresponding to $\Omega = 0$) of the formation of the additional branch (and the minimum lasing threshold). If $I_4^0 = 0$, the branches $f(x)$, as demonstrated by Eq. (3.8), obey the equations

$$f = |\Delta|, \ \mathrm{th}(fx) = f \geqslant |\Delta|. \tag{3.11}$$

We can see from Fig. 3a that an increase in the nonlinear parameter x may result in a smooth transition from the main branch to an additional (lasing) branch of the solution. This corresponds to "soft" lasing. The main and additional branches diverge (Fig. 3a) for any value $I_4^0 \neq 0$ no matter how small. Therefore, the additional branch can be regarded as the lasing curve "disturbed" by the beam 4.

It follows from general considerations that, no matter how small the value of I_4^0, the approximation of constant pumping ceases to be valid sooner or later as x approaches x_{cr}, which is demonstrated clearly in Fig. 3a. The value of $M_{34}(x)$ reaches saturation as the waves 1 and 2 are depleted. Using Eq. (3.8) corresponding to $I_4^0 \ll 1$ and $|x - x_{cr}| \ll x_{cr}$, we can investigate the behavior of closely spaced branches of $|c(x)|^2$ and determine the range of validity of the constant pumping approximation. It is then found that for larger x_{cr} on increase in I_4^0 obeys the law $\delta x_{cr} \propto (I_4^0)^{1/3}$, i.e., the increase is very rapid. The order of magnitude of δx_{cr} is given by the separation between the main and additional branches. The condition of validity of the constant pumping approximation is then $(x_{cr} - x)/x_{cr} \gg (I_4^0)^{1/3}$. This is a very stringent condition.

The behavior of an additional branch for $\Gamma < 0$ is clearly unrelated to lasing. The values of $|\Gamma l|_{cr}$ are in this case relatively high (Fig. 3d) and they increase rapidly as the width of the branch $f_1 - f_2 = 2[(I_4^0 - I_1^0)^2 - |\Delta|]^{1/2}$ increases.

Reflection coefficient of a reversed wave

We shall use the results obtained for branches of $|c(x)|^2$ to calculate the observed characteristic M_{34}. The general expression for $M_{34}(x)$ obtained for $\Omega = 0$ from Eq. (3.2) is

$$M_{34} = (1 - f^2)[1 - f \,\mathrm{cth}\,(fx)]^{-2}. \tag{3.12}$$

In the limit of large values of the interaction parameter $x \to \pm\infty$, we find that $M_{34} = (1 \pm f)/(1 \mp f)$. Obviously, we have $M_{34}(\infty) \geqslant 1$ and $M_{34}(-\infty) \leqslant 1$. In Eq. (3.12) we should substitute the appropriate values of $f(x)$. In the case of the main branch we find from Eq. (3.10) that

$$M_{34}^{(0)}(\infty) = I_1^0 I_2^l / I_4^0 (1 - I_2^l). \tag{3.13}$$

An increase in I_2^l and in the ratio I_1^0/I_4^0 results in a monotonic increase of the reversal coefficient $M_{34}^{(0)}(\infty)$. It should be stressed that M_{34} has no upper limit because energy is acquired from the pump waves. It can also be shown that when x is increased, the limiting value given by Eq. (3.13) is attained monotonically when the values of I_1^0, I_2^l, and I_4^0 are fixed. Figure 4 shows the dependence of M_{34} on $\Delta \equiv 2I_2^l - 1$ for various values of the interaction parameter. Already for $x \approx 0.8$ the dependence $M_{34}(\Delta)$ is strongly asymmetric and

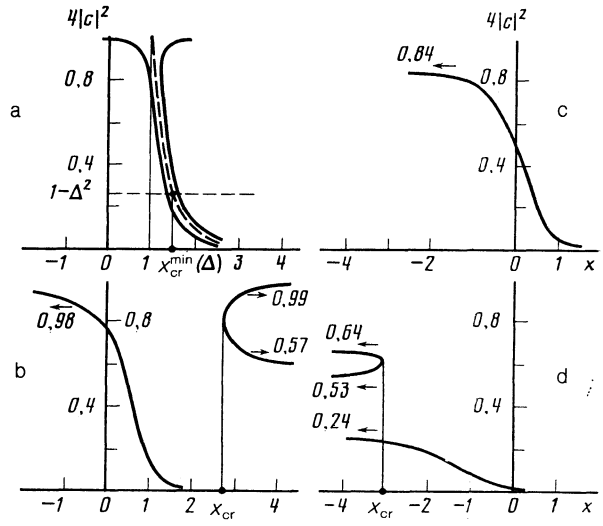

FIG. 3. Branches of the function $4|c|^2(x)$ obtained for different input parameters. The dashed curve in Fig. 3a corresponds to $I_4^0 = 0$ [see Eq. (3.8)]. The lasing curve corresponds to $x > x_{cr}^{min}(\Delta)$. Parameters: a) $I_1^0 = 0.499$, $I_2^l = 0.5$, $I_4^0 = 0.001$, $\Delta = 0$; b) $I_1^0 = 0.35$; $I_2^l = 0.55$, $I_4^0 = 0.1$, $\Delta = 0.1$; c) $I_1^0 = 0.4$, $I_2^l = 0.3$, $I_4^0 = 0.3$, $\Delta = -0.4$; d) $I_1^0 = 0.01$, $I_2^l = 0.2$, $I_4^0 = 0.79$, $\Delta = -0.6$.

is not described by the constant pumping approximation.

The limiting values $M_{34}(\infty)$ for the additional branch are easily obtained from the limiting values of f found earlier. The ratio of the values of M_{34} for the main and additional branches can be arbitrary and depends on the relationship between the quantities I_1^0, I_2^l, I_4^0. In other words, the function $M_{34}(x)$ calculated for the main branch may intersect the function $M_{34}(x)$ for the additional branch. Naturally, the branches of $|c(x)|^2$ do not intersect.

We shall now consider in greater detail the reversal coefficient M_{34} for an additional branch in the case when the

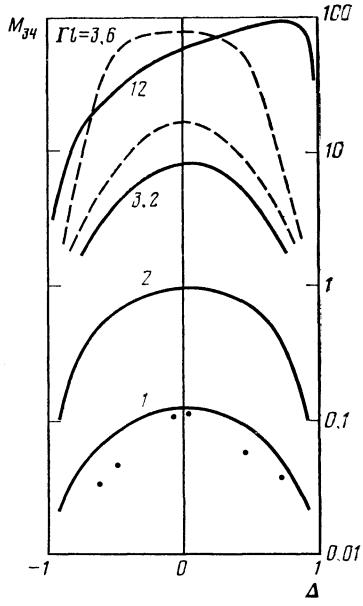

FIG. 4. Dependences of the reflection coefficient M_{34} on Δ plotted for different values of the interaction parameter. The dashed curves represent the constant pumping approximation. In the case of $\Gamma l = 1$ and 2 the difference between the exact and approximate solutions is negligible. The points represent the experimental results. The value $\Gamma l = 3.2$ corresponds to the lowest dashed curve.

signal wave 4 is weak. Substitution of the values of $f^{(1,2)}$ found above gives

$$M_{34}^{(1)}=(1+\Delta)/2I_4^0, \quad M_{34}^{(2)}=(1+|\Delta|)/(1-|\Delta|). \quad (3.14)$$

Usually the intensities of the pump beams are given by $I_1^0 \propto I_2^l$. Then, we find that $M_{34}^{(1)} \gg M_{34}^{(2)} > 1$. If terms up to I_4^0 are included, then $M_{34}^{(1)} = M_{34}^{(0)}$.

Stability of stationary solutions

The existence of triple-valued stationary solutions makes it necessary to consider the problem of stability. In the case of a purely nonlocal response it is possible to investigate the stability of the actual wave amplitudes against small perturbations on the basis of the time-dependent equations (2.2) and (2.3) (see the Appendix). The results of this investigation are as follows. A stationary solution corresponding to the main branch of $|c(x)|^2$ is stable against small perturbations. The additional double-valued branch of $|c(x)|^2$ always has a point corresponding to an instability threshold near the bottom of the parabola (Fig. 3) and it separates the stable from the unstable parts. The stable part of the additional branch reduces in the limit $I_4^0 \to 0$ to the lasing curve (Fig. 3a).

It therefore follows that in the ranges of the input parameters shown in Fig. 2 we can have both stable and bistable solutions. The nature of the transient process determines which of the bistable solutions is observed experimentally.

§4. OPTICAL-FREQUENCY LASING

Several lasing regimes are possible when one or two noninteracting beams are incident on a crystal. If the nonlinear parameter is greater than a certain threshold value, three or two coupled secondary waves are formed and these can be detected at the exit from a crystal. In this section we consider above-threshold stationary states corresponding to different types of boundary conditions.

Mirror-free regime

This regime corresponds to the boundary conditions $I_4^0 = I_3^l = 0$ (Fig. 1b). The waves 1 and 2 represent the pump. The threshold value of the interaction parameter x_{cr} and the dependence $f(x)$ are described respectively by Eqs. (3.7) and (3.11). The output intensities of the lasing beams $I_3^0 \equiv I_3(0)$ and $I_4^l \equiv I_4(l)$ can be expressed directly in terms of $f(x)$ using the conservation laws (2.5). If $x > x_{cr}$, then

$$I_3^0=\frac{f^2-\Delta^2}{2(1-\Delta)}, \quad I_4^l=\frac{f^2-\Delta^2}{2(1+\Delta)}. \quad (4.1)$$

The polarization of the output beams is orthogonal to the polarization of the pump waves. We can see from Eq. (3.11) and also from Fig. 3a that if $\Omega = 0$, then above the lasing threshold the quantity $f \equiv (1-4|c|^2)^{1/2}$ increases from $|\Delta|$ to unity. Then, the values of I_3^0, I_4^0 increase monotonically from zero to the limiting values $I_3^0 = I_2^l$ and $I_4^l = I_1^0$. It follows that the energy of the pump beams is transferred completely to the waves 3 and 4 if Γl is sufficiently large. This is a consequence of unidirectional energy exchange. If $\Delta = 0$, i.e., if the pumping is symmetric, the lasing characteristics of the waves 3 and 4 are also symmetric.

If $\Delta = 0$, lasing is possible for an arbitrary ratio of Γ and Ω. As pointed out in §3, the lasing threshold is now less than for $\Omega = 0$ and $\Delta = 0$. The behavior above the threshold can be investigated using Eqs. (3.3) and (4.1). It remains qualitatively the same as for $\Omega = 0$ and $\Delta \neq 0$.

We shall stress once again the soft nature of the excitation of secondary waves and the fact that such a regime cannot occur in the diffusive nonlinearity mechanism. It should also be pointed out that the part of the branch $f = |\Delta|$ when $x > x_{cr}$, which corresponds to an unperturbed state above the lasing threshold, is unstable against the growth of the waves 3 and 4. This follows from general physical considerations.

Mirror regime

This regime corresponds to boundary conditions of a new type. Let us assume that these conditions are

$$I_1^0=R_1I_2^0, \quad I_2^l=R_2I_1^l, \quad I_3^l=0, \quad I_4^0 \neq 0, \quad (4.2)$$

where $R_{1,2}$ are the reflection coefficients of mirrors in a resonator (Fig. 1c). The pumping is provided by the ordinary wave 4. The subthreshold regime corresponds to $I_1 = I_2 = I_3 = 0$ and $I_4 = I_4^0$. Above the lasing threshold, we have $I_{1,2,3} \neq 0$. In this regime a crystal can be regarded as a passive reversing mirror, characterized by the reversal coefficient $M_{34} = |A_{34}(0)|^2$.

The change of the polarization of the wave 4 to ordinary, i.e., the substitution of $\Gamma \to -\Gamma$ in the main equations of the system (2.7) is simply a matter of convenience. In Fig. 1c in terms of the notation adopted by us in Eq. (2.10) the lasing regime corresponds to $\Gamma > 0$. However, if the pumping were provided by the e wave, we would have $\Gamma < 0$.

A complete investigation of the nonlinear behavior can be carried out on the basis of the general solution of Eq. (2.8). As in §3, our task is to use algebraic equations to find the integration constants D_{12} and D_{34} and the conserved quantities c and $d_{1,2}$ (or Δ and Σ). In contrast to the preceding case, none of the quantities c, Δ, Σ, or $d_{1,2}$ is determined simply by the boundary conditions.

Using the self-evident identities $|c|^2R_2 = (I_2^l)^2$ and $I_2^l = (\Delta+1)/2$, we readily obtain the following algebraic relationship from Eqs. (2.8) and (4.2):

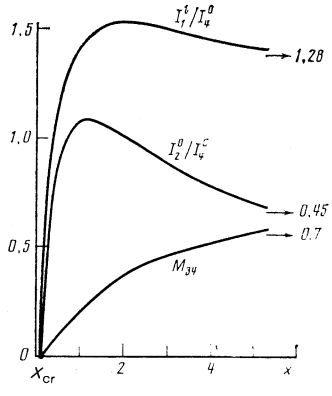

FIG. 5. Normalized intensities of output beams and the reflection coefficient for a reversed wave in the lasing regime plotted as a function of the interaction parameters.

$$\left| \frac{(\Gamma\Delta - i\Omega)T + [(\Gamma - i\Delta\Omega)^2 - R_2^{-1}z^2(\Gamma^2+\Omega^2)]^{1/2}}{[(\Gamma - i\Omega\Delta) - R_2^{-1}(\Gamma + i\Omega)z]T + [(\Gamma - i\Omega\Delta)^2 - R_2^{-1}z^2(\Gamma^2+\Omega^2)]^{1/2}} \right|^2 = R_1R_2, \tag{4.3}$$

where

$$T \equiv \text{th}\{l[(\Gamma - i\Omega\Delta)^2 - R_2^{-1}z^2(\Gamma^2+\Omega^2)]^{1/2}/4\}, \quad z \equiv \Delta + 1.$$

In principle, the above relationship can be used to find Δ as a function of Γl and Ωl. Knowing Δ, we can calculate the reversal coefficient M_{34}:

$$M_{34} = \frac{(\Omega^2+\Gamma^2)z^2|T|^2}{R_2|(\Omega\Delta + i\Gamma)T + [(\Gamma - i\Omega\Delta)^2 - R_2^{-1}z^2(\Gamma^2+\Omega^2)]^{1/2}|^2}. \tag{4.4}$$

The output intensities of the lasing beams 1 and 2 can be expressed in terms of I_4^0 using the formulas

$$I_2^0 = \frac{[z - (2-z)M_{34}]I_4^0}{2 - z(1+R_1)}, \quad I_1^l = \frac{z(1 - R_1M_{34})I_4^0}{R_2[2 - z(1+R_1)]}. \tag{4.5}$$

In the case of a purely local response, i.e., when $\Gamma = 0$, Eqs. (4.3) and (4.4) are identical with the corresponding formulas given in Ref. 3. In this case there is no lasing: $I_{1,2,3} = M_{34} = 0$.

We shall find first the lasing threshold on the basis of Eq. (4.3). At the threshold, we have $I_1 = I_2 = 0$, i.e., $z \equiv \Delta + 1 = 0$. We shall also obtain the expected relationship $(\Gamma l)_{cr} = -\ln(R_1R_2)$. This relationship can easily be modified to include the bulk losses also. We can see that lasing is due to a nonlocal response, i.e., due to the circular photogalvanic effect.

We shall now investigate a nonlinear response corresponding to $\Omega = 0$. Equation (4.3) then separates into two independent equations:

$$\frac{\text{th}(\bar{f}x)}{\bar{f}} = \frac{1 \mp (R_1R_2)^{1/2}}{1 - z \pm (R_1R_2)^{1/2}(1 - R_2^{-1}z)}, \qquad \bar{f} = (1 - R_2^{-1}z^2)^{1/2}, \quad x \equiv \frac{\Gamma l}{4}. \tag{4.6}$$

These equations differ greatly from those obtained in Ref. 3 for the diffusive nonlinearity. We can show that the equation corresponding to the lower sign in Eq. (4.6) has no physical solutions, i.e., it has no solutions with $I_{1,2,3} > 0$. However, the equation corresponding to the upper sign always has a single-valued physical solution. Above the lasing threshold, i.e., in the range $x \geqslant x_{cr}$, the value of Δ rises monotonically from $\Delta[x_{cr}) = -1$ to $\Delta(\infty) = -(1 - R_2)/(1 + R_2)$ for $R_2 \leqslant R_1$ or to $\Delta(\infty) = -[1 - 2(R_1R_2)^{1/2}/(1 + R_1)]$ for $R_1 \leqslant R_2$. The reversal coefficient increases correspondingly from $M_{34}(x_{cr}) = 0$ to

$$M_{34}(\infty) = \min(R_{1,2}). \tag{4.7}$$

The maximum value of M_{34} is determined by the smallest of the mirror reflection coefficients. As expected, the energy flux is directed to the right, i.e., $\Delta < 0$.

The behavior of $I_1^l(x)$ and $I_2^0(x)$ depends on the relationship between R_1 and R_2. If $R_2 < R_1$, then $I_2^0(x)$ reaches a maximum and falls to zero, whereas $I_1^l(x)$ rises monotonically, approaching $I_1^l(\infty) = I_4^0$. If $R_2 > R_1$ then all the limiting intensities of the lasing beams are finite:

$$I_2^0(\infty) = I_4^0 R_1^{1/2}(R_2^{1/2} - R_1^{1/2})/[1 - (R_1R_2)^{1/2}],$$
$$I_1^l(\infty) = I_4^0 R_1^{1/2}(1 - R_1)/R_2^{1/2}[1 - (R_1R_2)^{1/2}]. \tag{4.8}$$

The functions $I_1^l(x)$ and $I_2^0(x)$ reach the limiting values of Eq. (4.8) by generally nonmonotonic processes. Figure 5 shows the results of numerical calculations. It is worth noting the rapid rise of I_1^l and I_2^0 in the initial region beyond the lasing threshold and the slow attainment of the limiting value. Therefore, the intensity of the opposite lasing beam I_2^0 is low compared with the intensity of the forward beam I_1^l.

It follows from the above expressions that lasing disappears if even one of the mirror reflection coefficients vanishes. This property is specific to the nonlinearity mechanism being investigated. In the diffusion mechanism, we can expect lasing for $R_1 = 0$ (semilinear reversing mirror[3]).

Finally, we must point out that other mirror lasing regimes may be based on the photogalvanic nonlinearity and these have boundary conditions different from those given by Eq. (4.2) (see, for example, Fig. 1d). However, an analysis of these regimes is outside the scope of the present paper.

§5. EXPERIMENTS

Experiments were carried out on iron-doped lithium niobate crystals. Samples with x and y cuts and several millimeters thick were used. The concentration of iron amounted to a few hundredths of 1 wt.%.

The radiation sources were helium–cadmium (0.44 μm) and argon (0.45–0.51 μm) lasers.

The precision of orientation of the **c** axis relative to the faces of a sample was 5′ and the plane of convergence of the beams was set relative to this axis to within 1°. These precautionary measures were taken in order to avoid or weaken considerably the influence of the usual recording (grating-formation) mechanism associated with the photocurrents $\mathbf{j}_{ph} \| \mathbf{c}$. A calibration experiment, which confirmed that this mechanism was practically completely suppressed, involved determination of the state of polarization of a beam diffracted by a recorded grating. The polarization of this beam was orthogonal relative to the polarization of the "read" beam to within 0.1%.

The diffraction efficiency of 10% was readily attained for a sample 3 mm thick.

Two-beam interaction

An investigation of the kinetics of changes in the intensities of interacting beams in accordance with the geometry shown in Fig. 1a demonstrated that, irrespective of the input values $I_{e,o}(0)$, the intensity of the extraordinary wave at the output increased, whereas the intensity of the ordinary wave decreased. The direction of energy exchange was not affected by rotation of the crystal by 180° relative to the **c** axis or one of the transverse axes. Therefore, the antisymmetric component of the photogalvanic tensor β_a of Eq. (1.4) should be regarded as negative ($\beta_a < 0$). The results of a direct experiment on the two-beam interaction confirmed the predicted existence and the relatively large magnitude of the circular photogalvanic effect in $LiNbO_3$, deduced from

an investigation of the spontaneous transformation of modes, differing in their polarization in fiber waveguides,[17] and also from the light-induced polarization anisotropic scattering.[18]

The fact that even a weak o wave ($I_o/I_e \approx 10^{-2}$) decayed linearly with time while a grating was being written led us to the conclusion that there was no transient energy exchange associated with the local nonlinear mechanism (see §1). Hence, in the case of $LiNbO_3$:Fe we found that $\beta_a \gg \beta_s$; this was in agreement with the experimental estimate of the ratio β_a/β_s made in Ref. 19.

Prolonged exposures of $LiNbO_3$:Fe crystals to laser radiation resulted in the development of significant light-induced scattering,[20] which was responsible for part of the energy of the interacting beams; moreover, the wavefronts were distorted because of the appearance of a strong nonlinear lens.[21] These processes make it difficult to compare quantitatively the theoretical and experimental results for stationary states.

Opposed four-wave interaction

When two opposite o waves were used for the purpose of pumping and a signal e wave was introduced in a plane perpendicular to the **c** axis ($\Gamma > 0$), a wave was produced which was reversed relative to the signal wave. It was polarized in the same way as the signal wave and was orthogonal to the pump waves. A change in the wave polarizations (corresponding to an e pump wave, an o signal wave, and $\Gamma < 0$) reduced the reversal coefficient M_{34} considerably (from 11 to 4% for one of the samples).

When unfocused laser beams were used, the constant pumping approximation remained valid. The maximum value of M_{34} was observed, in agreement with Eq. (3.5), when the intensities of the pump waves were equal, $\Delta = 0$, as shown in Fig. 4.

The measured steady-state values of the reversal coefficient were always smaller than those calculated using the values of the gain Γ determined for the two-beam interaction. The maximum recorded steady-state value of the reversal coefficient was $M_{34} \approx 0.3 < 1$. On the other hand, in the presence of an additional mirror, it was possible to achieve lasing in the same sample (Fig. 1d) inside a resonator formed by the crystal itself and the additional mirror. The appearance of a lasing beam was a clear demonstration that the reversal coefficient exceeded unity. The reason for this could be that in the lasing regime an output wave could become adjusted in an optimal manner to the pump wave both in respect of the direction and the structure of the wavefront (the pump beams had a limited cross section, Gaussian profiles, and optical inhomogeneities). However, the use of a Gaussian signal wave oriented precisely on a crystal and characterized by the same cross section as that of the pump beams prevented such self-adjustment.

The competing nonlinearity of the self-focused field prevented high values of the parameter $\Gamma l/4$ from being attained in lithium niobate in the range where multivalued solutions and optical bistability were predicted theoretically. However, in the case of small values of $x = \Gamma l/4$ there was qualitative agreement between the theory and experiment.

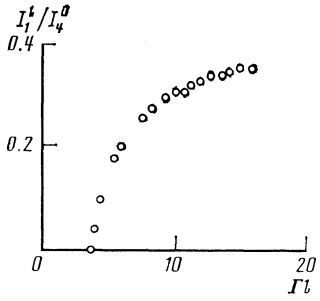

FIG. 6. Dependence of the normalized intensity of the lasing wave on the interaction parameter obtained for a 0.3 cm thick iron-doped lithium niobate crystal (0.02 wt.% Fe); $R_{1,2} = 0.16$.

Lasing in a linear resonator

It was reported in Refs. 22 and 23 that when an ordinary wave was used to pumping a crystal with plane-parallel ends polished to give optical surface quality, lasing e beams and a reversed o wave were generated. In this case the opportunity for self-adjustment of the wavefronts and optimization of the four-wave interaction was clearly the greatest, since a single pump wave created three additional waves: two lasing waves and one reflected wave (Fig. 1c).

Once again the experimental results were in good agreement with calculations. Firstly, a self-excitation threshold was observed: lasing appeared only beginning from a certain angle of incidence of the pump beam on a sample. This was associated with a strong rise of the gain at low angles, predicted by Eqs. (1.13) and (1.14). Secondly, when the reflection coefficients of the resonator mirrors were equal (identical reflection by the crystal ends, $R = 16\%$) the output lasing beams were very different in intensity: the forward beam obtained in the saturation regime carried more than 35% of the pump beam intensity and the opposite beam represented less than 2% of this intensity. Thirdly, the output energy of the forward lasing beam increased, in accordance with calculations, as the interaction constant increased above the threshold value (Fig. 6).

A method described in Ref. 23 was used to carry out measurements of the threshold value of the gain Γ_{th} of iron-doped lithium niobate for several specific lines emitted by argon and helium–cadmium lasers. Figure 7 shows the spectrum of the gain Γ representing the spectral dependence of the antisymmetric component of the photogalvanic tensor β_a. The values of Γ corresponded to a power density of the pump beam of $\sim 10^3$ W/cm^2 in the sample (argon laser radiation beam focused on the sample). The spectrum of Γ was qualitatively similar to the absorption spectrum of divalent

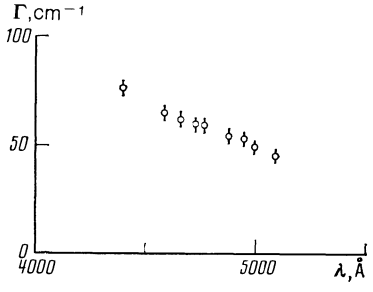

FIG. 7. Spectrum of the gain Γ for a lithium niobate crystal activated with 0.02 wt.% Fe.

iron in lithium niobate and this impurity is usually assumed to form active photogalvanic centers.

CONCLUSIONS

Equations describing a four-wave polarization interaction in photorefractive crystals have been derived. This interaction is due to linear and circular photogalvanic currents; its properties are different from those of the interaction associated with the drift and diffusion of photoelectrons. The exact solutions of the nonlinear equations describing various experimental geometries were obtained. Multistability of the solutions has been established and its distinguishing features identified; the stability of multistable solutions has been studied. Optical-frequency lasing due to the photogalvanic nonlinearity has been studied and the characteristics of lasing beams above the threshold, as well as of the reflection coefficient of a reversed wave, were determined.

Phase conjugation has been achieved in $LiNbO_3$:Fe crystals and frequency-degenerate optical-frequency lasing has been obtained in linear and semiopen resonators. The experimental results are in qualitative agreement with the calculations; a strong competing nonlinearity of the self-focusing type made it difficult to carry out a quantitative comparison in the steady-state case. Measurements of the threshold angles for lasing were used in a calculation of the gain spectrum, which gave information on the spectrum of the circular component of the photogalvanic tensor.

Investigations of the effects of the giant photorefractive nonlinearity are of obvious scientific and practical importance. The known interaction mechanisms are already used in several important applications.[24-26] The discovery and investigation of a new type of interaction offers new opportunities for applications.

APPENDIX

In the case of a nonlocal response ($F' = 0$) the real nature of the initial equations (2.2) and (2.3) justifies the assumption that the amplitudes a_i are also real: Using the conservation laws of Eq. (2.5), we shall adopt the θ, φ phase representation:

$$a_1=d_1^{1/2}\cos\theta, \quad a_2=d_2^{1/2}\cos\varphi, \quad a_3=d_2^{1/2}\sin\varphi; \quad a_4=d_1^{1/2}\sin\theta. \tag{A.1}$$

Instead of Eq. (2.3), we now obtain $d\theta/dy = d\varphi/dy = -G$. The phase shift independent of y $\alpha_0 = \varphi - \theta$ can be expressed in terms of c and c_2:

$$c=(d_1d_2)^{1/2}\cos\alpha_0, \quad c_2=(d_1d_2)^{1/2}\sin\alpha_0. \tag{A.2}$$

Introducing a new angular variable $\psi = \varphi + \theta$, we can finally write down the initial system of equations in the following simple form;

$$\frac{d\psi}{dy} = -2G, \quad \left(\frac{\partial}{\partial\tau}+1\right)G = \frac{f}{2}\sin(\psi+\psi_0), \tag{A.3}$$

where $f=(1-4c^2)^{1/2}$, $\sin\psi_0 = f^{-1}\sin\alpha_0$, and $\cos\psi_0 = f^{-1}\Delta\cos\alpha_0$ are y-independent quantities. The boundary conditions for ψ are

$$\psi(0,\tau)=2\theta_0+\alpha_0, \quad \psi(l)=-\alpha_0, \tag{A.4}$$

where $\alpha_0=\alpha_0(\tau)$, whereas $\theta_0\equiv\theta(0)$ is a constant determined, in accordance with Eq. (A.1), by the input amplitudes $a_{1,4}(0)$.

Assuming that the perturbations of ψ, G, and α_0 relative to their steady-state values are proportional to $\exp(\nu\tau)$, we find that the instability growth rate ν is described by

$$(\nu+1)\frac{d}{dx}\delta\psi = A\delta\psi + B\delta\psi(0), \quad \delta\psi(0) = -\delta\psi(l). \tag{A.5}$$

The quantity $A(x)$ and $B(x)$ can be expressed in terms of the stationary solution $\psi(x)$:

$$A=-f\cos(\psi+\psi_0), \qquad B=-\frac{f}{2\Delta}[(1+\Delta^2)\cos(\psi+\psi_0)+(1-\Delta^2)\cos(\psi-\psi_0)]. \tag{A.6}$$

It follows from Eq. (A.3) that $\psi(x)$ satisfies the algebraic equation

$$\mathrm{tg}[(\psi+\psi_0)/2] = \mathrm{tg}[\theta_0+(\alpha_0+\varphi_0)/2]\exp(-2fx). \tag{A.7}$$

We can demonstrate the identity of Eqs. (A.7) and (3.8). Integrating Eq. (A.5) with the aid of Eq. (A.7) and assuming $\nu = 0$, we find after algebraic transformations that

$$f^2+\Delta+(f^2+\Delta)\frac{\sin(2\theta_0+\alpha_0+\psi_0)}{\sin(\psi_0-\alpha_0)} = 8fxcc_2\sin(2\theta_0+\alpha_0+\psi_0). \tag{A.8}$$

The system of transcendental equations (A.7), (A.8) determines the threshold point x_{th} for each of the single-valued branches $\alpha_0(x)$ [or, equivalently, for each of the branches $c(x)$].

By means of graphical analysis, we can show that in the case of the main branch $\alpha_0(x)$ [or $c(x)$] Eq. (A.8) has no solutions. In other words, the main branch is stable against small perturbations. In the case of an additional double-valued branch $\alpha_0(x)$, we find that there is always a unique solution. Calculations show that the point x_{th} is located in the direct vicinity of the base of the parabola, i.e., $x_{th} \approx x_{cr}$ (Fig. 3). In the limit $I_4^0 \to 0$ the unstable part of the additional branch corresponds to the unperturbed state of two pump waves above the lasing threshold (see §3).

The authors are grateful to B. Ya. Zel'dovich for a valuable discussion of their results and to A. I. Chernykh for numerical calculations.

Note added in proof (May 22, 1987). Mirror-free lasing, similar to that predicted in the present study, was observed recently by A. D. Novikov, V. V. Obukhovskiĭ, S. G. Odulov, and B. I. Sturman [Pis'ma Zh. Eksp. Teor. Fiz. **44**, 418 (1986); JETP Lett. **44**, 538 (1986)].

[1] V. M. Fridkin, *Photoferroelectrics*, Springer Verlag, Berlin (1979).
[2] V. L. Vinetskiĭ, N. V. Kukhtarev, S. G. Odulov, and M. S. Soskin, Usp. Fiz. Nauk **129**, 113 (1979) [Sov. Phys. Usp. **22**, 742 (1979)]; N. V. Kukhtarev, V. B. Markov, S. G. Odulov, M. S. Soskin, and V. L. Vinetskiĭ, Ferroelectrics **22**, 949 (1979).
[3] M. Cronin-Golomb, B. Fischer, J. O. White, and A. Yariv, IEEE J. Quantum Electron. **QE-20**, 12 (1984).
[4] M. P. Petrov, S. I. Stepanov, and A. V. Khomenko, Photo-sensitive Electrooptic Media in Holography and Optical Image Processing [in Russian], Nauka, Leningrad (1983).
[5] B. Ya. Zel'dovich, V. V. Shkunov, and N. F. Pilipetskiĭ, Phase Conjugation [in Russian], Nauka, Moscow (1985).
[6] F. S. Chen, J. Appl. Phys. **38**, 3418 (1967).
[7] J. J. Amodei, Appl. Phys. Lett. **18**, 22 (1971).

[8]A. M. Glass, D. von der Linde, and T. J. Negran, Appl. Phys. Lett. **25**, 233 (1974).
[9]V. I. Belinicher and B. I. Sturman, Usp. Fiz. Nauk **130**, 415 (1980) [Sov. Phys. Usp. **23**, 199 (1980)].
[10]B. I. Sturman, Zh. Eksp. Teor. Fiz. **83**, 1930 (1982) [Sov. Phys. JETP **56**, 1116 (1982)].
[11]V. I. Belinicher, Phys. Lett. A **66**, 213 (1978).
[12]B. I. Sturman, Kvantovaya Elektron. (Moscow) **7**, 483 (1980) [Sov. J. Quantum Electron. **10**, 276 (1980)].
[13]S. G. Odulov, Pis'ma Zh. Eksp. Teor. Fiz. **35**, 10 (1982) [JETP Lett. **35**, 10 (1982)].
[14]N. V. Kukhtarev, Pis'ma Zh. Tekh. Fiz. **2**, 1114 (1976) [Sov. Tech. Phys. Lett. **2**, 438 (1976)].
[15]B. I. Sturman, Zh. Tekh. Fiz. **48**, 1010 (1978) [Sov. Phys. Tech. Phys. **23**, 589 (1978)].
[16]S. I. Stepanov and M. P. Petrov, Opt. Commun. **53**, 64 (1985).
[17]S. I. Bozhevol'nyĭ, E. M. Zolotov, P. G. Kazanskiĭ, A. M. Prokhorov, and V. A. Chernykh, Pis'ma Zh. Tekh. Fiz. **9**, 690 (1983) [Sov. Tech. Phys. Lett. **9**, 297 (1983)].
[18]E. M. Avakyan, K. G. Belabaev, and S. G. Odulov, Fiz. Tverd. Tela (Leningrad) **25**, 3274 (1983) [Sov. Phys. Solid State **25**, 1887 (1983)].
[19]P. G. Kazanskiĭ, A. M. Prokhorov, and V. A. Chernykh, Pis'ma Zh. Eksp. Teor. Fiz. **41**, 370 (1985) [JETP Lett. **41**, 451 (1985)].
[20]I. F. Kanaev, V. K. Malinovskii (Malinovsky), and B. I. Sturman, Opt. Commun. **34**, 95 (1980).
[21]A. Ashkin, G. D. Boyd, J. M. Dziedzic, R. G. Smith, A. A. Ballman, J. J. Levinstein, and K. Nassau, Appl. Phys. Lett. **9**, 72 (1966).
[22]S. G. Odulov and M. S. Soskin, Pis'ma Zh. Eksp. Teor. Fiz. **37**, 243 (1983) [JETP Lett. **37**, 289 (1983)].
[23]S. G. Odulov, Kvantovaya Elektron. (Moscow) **11**, 529 (1984) [Sov. J. Quantum Electron. **14**, 360 (1984)].
[24]B. Fischer and S. Sternklar, Appl. Phys. Lett. **47**, 1 (1985).
[25]M. D. Ewbank and P. Yeh, Opt. Lett. **10**, 496 (1985).
[26]A. E. Chiou and P. Yeh, Opt. Lett. **11**, 306 (1986).

Translated by A. Tybulewicz